LAWRENCE
LIVERMORE
NATIONAL
LABORATORY

UCRL-CONF-212717

Neutron Source Strength Estimates from (a, n) Reactions in Binary Mixtures of Actinide Particles and Light Element Particles

J. L. Boles, R. S. Hafner, L. E. Fischer

June 6, 2005

2005 ASME Pressure Vessels and Piping Division Conference
Denver, CO, United States
July 17, 2005 through July 21, 2005

Disclaimer

Proceedings of PVP2005
2005 ASME Pressure Vessels and Piping Division Conference
July 17-21, 2005, Denver, Colorado USA

PVP2005-71741

NEUTRON SOURCE STRENGTH ESTIMATES FROM (α, n) REACTIONS IN BINARY MIXTURES OF ACTINIDE PARTICLES AND LIGHT ELEMENT PARTICLES*

Jason L. Boles
Ronald S. Hafner
Larry E. Fischer
Risk and Response Management Program
Lawrence Livermore National Laboratory
P.O. Box 808, Livermore, CA 94550 USA
E-mail: boles1@llnl.gov

INTRODUCTION

This paper describes an example of a model used to estimate the neutron source term from (α, n) reactions from a mixture of PuO_2 and BeO particles. The (α, n) reaction occurs when an α-particle, emitted by an actinide isotope such as ^{239}Pu, collides with, and is absorbed by, the nucleus of a light element such as beryllium. Neutrons are produced through the reaction

$$ {}^{4}_{2}\alpha + {}^{9}_{4}\mathrm{Be} \rightarrow {}^{12}_{6}\mathrm{C} + {}^{1}_{0}n \,. \qquad (1) $$

This reaction is commonly abbreviated as $^{9}Be(\alpha, n)^{12}C$, or just Be(α, n).

This binary mixture of actinide oxide particles and oxide particles of light elements is proposed for a payload to be shipped in the 9975 Package (the 9975). The 9975 is a Type B package certified by the U.S. Department of Energy (DOE, 2004a). The package is evaluated against the requirements of Title 10, Code of Federal Regulations, Part 71 (10 CFR 71), *Packaging and Transportation of Radioactive Material* (NRC, 1995), as documented in *Safety Analysis Report for Packaging Model 9975 B(M)F-85* (WSRC, 2003) (the 9975 SARP), as required by DOE Order 460.1B, *Packaging And Transportation Safety* (DOE, 2003).

To add an authorized payload to a certified package, the applicant must show in the safety analysis report for packaging, through analysis or testing, that the packaging with the proposed contents meets the requirements for packages of radioactive material in 10 CFR 71. Specifically, 10 CFR 71.47 requires that the dose rate at any point on the external surface of the package not exceed 2 mSv/h (200 mrem/h), and that the dose rate 1 m from the external surface of the package not exceed 0.1 mSv/h (10 mrem/h). Exceptions to these dose rate limits are provided if the package is shipped by exclusive use; however, the carrier used to ship these packages prefers that they not be shipped by exclusive use.

Preliminary calculations using commonly used computer programs (e.g., *SOURCES* [Wilson, 1999]) modeled this mixture of PuO_2 and BeO particles as a material homogeneously mixed at the atomic level. That model results in calculated neutron dose rates that are orders of magnitude higher than both measured in-facility dose rates and regulatory limits. Such a model is conservative because, physically, the

* This work was performed under the auspices of the U.S. Department of Energy by the University of California, Lawrence Livermore National Laboratory, under contract No. W-7405-Eng-48.

PuO_2 and BeO particles are not mixed at the atomic level, but rather at the particulate level.

This work models the mixture of PuO_2 and BeO particles as a material homogeneously mixed at the particulate level. Using such a model allows for some of the excess conservatism associated with atomic-level mixing to be removed. For example, historical PuO_2 particle size distribution measurements show that particle sizes range from tenths of microns to hundreds of microns (Thorp, 2001). Because the range of α-particles in PuO_2 is short, about 13 μm, the larger the PuO_2 particle, the greater the number of α-particles that get absorbed in the PuO_2 particle, and the lower the number of α-particles that escape the PuO_2 particle to potentially be absorbed by a beryllium atom.

The approach taken in this work is to estimate the (α, n) neutron source by multiplying:

- the rate that α-particles are produced by the actinide isotopes,
- the fraction of α-particles that escape the PuO_2 particles as a function of energy and particle size,
- the probability that an escaped α-particle would intersect a BeO particle, and
- the probability that an α-particle traveling in a BeO particle would undergo an (α, n) reaction.

Measured particle size distributions (Thorp, 2001) for 18 batches of plutonium oxides calcined according to DOE-STD-3013-2004 (DOE, 2004b), i.e., the 3013 Standard, at the Rocky Flats Environmental Technology Site were used and assumed to be representative of the oxides calcined there and elsewhere in the DOE complex. An example of the particle size distribution, from batch #0020, is shown in Fig. 1. The neutron source from (α, n) reactions was calculated for each of these particle size distributions, resulting in a distribution of neutron dose rates.

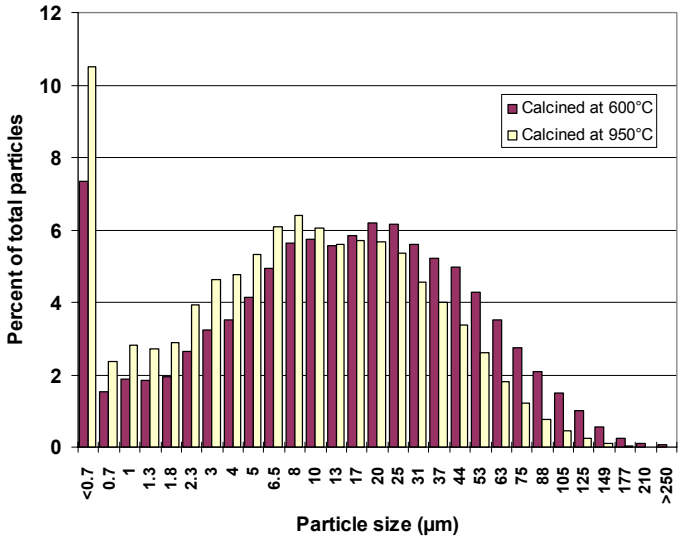

Figure 1. Particle Size Distribution by Number of Particles for Batch #0020.

CONTENT LIMITS

The contents of the 9975 package evaluated against the requirements of 10 CFR 71 are described in the 9975 SARP. Several different content envelopes are individually evaluated in the SARP. Content envelopes are differentiated by isotopic composition, chemical composition, composite materials, impurity amounts, etc. Content envelope C.4 consists of plutonium oxide, with up to a maximum of 4,400 g of radioactive material, up to a maximum of 500 g of Be, and up to a maximum of 5,000 g of all contents. Additional details of this and all other content envelopes can be found in Table 1.2 of the 9975 SARP.

Content envelope C.4 requires that the oxide contents be stabilized in accordance with Section 6.1.2 of the 3013 Standard: "Oxides shall be stabilized by heating the material in an oxidizing atmosphere to a Material Temperature of at least 950 °C (1,742 °F) for a time sufficient to meet the Stabilization Criteria in 6.1.2.3, but not less than 2 hours." The stabilization criterion in Section 6.1.2.3 of the 3013 Standard refers to the limit of 0.5% on the maximum moisture content of the oxide at the time of packaging. When subject to these stabilization conditions, beryllium forms BeO. Note that no Be-Pu-O compounds form below 1,400 °C (Levin, 1975), and, furthermore, the high-temperature intermetallic Pu-Be compound, $PuBe_{13}$, has not been observed under these conditions. Therefore, it is concluded that the particulate material does not include a homogeneous phase of plutonium and beryllium, which is consistent with the conclusion drawn from the difference between dose rate measurements and calculations based on a homogeneous mixture.

The limit of 4,400 g of Pu corresponds to 4,989 g of PuO_2. The limit of 500 g of Be corresponds to 1,388 g of BeO. The limit of 5,000 g of all contents prevents the maximum Pu and maximum Be from being shipped simultaneously in the same package. Thus, the mass of Be, the mass of Pu, or both, in a package must be reduced below their limits so that the mass of all contents does not exceed 5,000 g. Obviously, if the mass of Be is reduced to zero, the Be(α, n) neutron source will be zero. Equally as obvious, if the mass of Pu is reduced, the production rate of α-particles that can initiate the Be(α, n) reaction is also reduced. Therefore, it is necessary to iterate on the masses of Be and Pu to determine the combination within the loading constraints of the SARP that produces the maximum (α, n) neutron source and, hence, the maximum dose rate outside the package.

Note that, although BeO is described as an impurity in the 9975 SARP, it can in fact constitute a majority of the content by volume. At a theoretical density of 3.01 g/cm^3, 1,388 g of BeO (corresponding to 500 g of Be) occupies a volume of 461 cm^3. At a theoretical density of 11.46 g/cm^3, 4,989 g of PuO_2 (corresponding to 4,400 g of Pu) occupies a volume of 435 cm^3. In reality, it is likely that the cans of PuO_2 particles do not contain anywhere near 500 g of Be. Indeed, 500 g was selected as a maximum upper bound in the SARP because the exact amount of Be that may be present is unknown. The

difference in the mass of Be actually present in the cans and that assumed in these calculations is the primary source of uncertainty in the calculations.

ALPHA-PARTICLE GENERATION RATE

The first step in the process is to calculate the rate that α-particles are produced by the plutonium. This α-particle generation rate depends on both the mass of plutonium present and the isotopic distribution of plutonium isotopes.

The isotopic distribution is a factor, because the rate of decay (i.e., the activity, which is inversely proportional to the half-life) and the probability that the decay will result in the emission of an α-particle (i.e., the α-particle branching fraction) are dependent on the isotope. Table 1 shows the principal isotopes that are typically present in plutonium, along with their half-lives, their specific activities (i.e., the activity of 1 gram of that isotope), their α-particle branching fractions, and their specific α-particle generation rates.

Table 1. Properties of Plutonium Isotopes.

Isotope	Half-life (yr)	Specific Activity (Bq/g)	α-Particle Branching Fraction	Specific α-Particle Generation Rate ($\alpha \cdot s^{-1} \cdot g^{-1}$)
Pu-238	87.84	6.33E+11	1	6.33E+11
Pu-239	24,110	2.29E+09	1	2.29E+09
Pu-240	6,537	8.39E+09	1	8.39E+09
Pu-241	14.4	3.81E+12	2.45E-05	9.33E+07
Pu-242	376,000	1.46E+08	0.999995	1.46E+08
Am-241	432.2	1.27E+11	1	1.27E+11

Several plutonium isotopic distributions from the 3013 Standard are shown in Table 2. The Hanford distributions are representative of plutonium that has been "aged" for 10-30 years, and has experienced a significant buildup of ^{241}Am, and decay of ^{238}Pu and ^{241}Pu. For distributions in which the ^{241}Am content is larger than that in these representative distributions, the α-particle generation rate will be larger, but the total mass of radioactive material will be limited by the maximum 19 W decay heat limit specified in the 9975 SARP. The α-particle generation rate per gram of each plutonium isotopic distribution is shown below in Table 3.

Table 2. Isotopic Distribution (weight percent) of Representative Plutonium Distributions.

Isotope	Hanford 4-7% Pu-240	Hanford 10-13% Pu-240	Hanford 16-19% Pu-240
Pu-238	0.01	0.09	0.24
Pu-239	93.77	86.94	80.66
Pu-240	6	11.81	16.98
Pu-241	0.2	1	1.44
Pu-242	0.03	0.17	0.69
Am-241	0.14	0.86	2.8
Total	100.15	100.87	102.81

Note: For consistency with the 3013 Standard, the totals here do not add up to 100%.

Table 3. α-Particle Generation Rate per Gram of Plutonium ($\alpha \cdot s^{-1} \cdot g^{-1}$).

Isotope	Hanford 4-7% Pu-240	Hanford 10-13% Pu-240	Hanford 16-19% Pu-240
Pu-238	6.32E+07	5.65E+08	1.48E+09
Pu-239	2.15E+09	1.98E+09	1.80E+09
Pu-240	5.03E+08	9.83E+08	1.39E+09
Pu-241	1.86E+05	9.25E+05	1.31E+06
Pu-242	4.38E+04	2.46E+05	9.82E+05
Am-241	1.77E+08	1.08E+09	3.45E+09
Total	2.89E+09	4.61E+09	8.12E+09

ALPHA-PARTICLE ESCAPE FRACTION

The second step in the process is to calculate the fraction of α-particles that escape the PuO_2 particles.

Range, Initial Energy, and Threshold Energy

An α-particle, or any charged particle, moving through a material loses its kinetic energy through interactions with the electrons and nuclei of the material. The thickness of material that just stops a particle is called the *range* of the particle, and is dependent on the initial kinetic energy of the particle. Because the range of an α-particle in PuO_2 is short, about 13 μm, only those α-particles that are produced within range of the surface of the PuO_2 particle have a chance of escaping and interacting with a BeO particle to produce a neutron. Thus, it can be expected that, for a given PuO_2 mass, particle size distributions in which the average size of the PuO_2 particles is large will have a smaller fraction of α-particles that escape than distributions in which the average size of the PuO_2 particles is small, because a smaller fraction of α-particles produced are within range of the surface. In addition to the position in the PuO_2 particle where the α-particle is produced, the α-escape fraction is also dependent on the direction of travel of the α-particle.

The initial energy of the α-particle depends on the isotope from which it was produced and the energy state of the daughter product. Table 4 shows the energy released by the α-particle decay of the plutonium and americium isotopes (i.e., the Q values), and the energy of the highest intensity α-particle. Because the range of an α-particle is a function of its energy, multiple α-particle escape fractions would have to be calculated for each isotope. To simplify the calculation, a value of 5.6 MeV is used for the initial α-particle energy for all isotopes, which bounds the energy and, hence, the range of the α-particles emitted by the principal isotopes of plutonium. This is conservative, because the α-particle escape fraction for lower energies would be less, resulting in a lower (α, n) source term.

Table 4. α-Particle Decay Energy of Relevant Nuclides.

Isotope	α-Particle Decay Energy (MeV)	Principal α-Particle Energy (MeV)
Pu-238	5.593	5.499
Pu-239	5.245	5.157
Pu-240	5.256	5.168
Pu-241	5.140	4.896
Pu-242	4.984	4.900
Am-241	5.638	5.486

The nuclear reaction cross section for α-particle absorption by beryllium has a threshold energy below which no α-particles are absorbed. Hence, no neutrons are produced by (α, n) reactions by α-particles below this threshold energy. Figure 2 shows the cross section for the Be(α, n) reaction used in V 4C of the computer code *SOURCES* (Shores, 2004). The line labeled σ_T is the total neutron production cross section, and it has a definite threshold at about 1.5 MeV.

The distance t traveled by an α-particle from the point where it is produced with an initial energy, E_o, to the point at which its energy drops to some lower energy, E_α, is then simply the difference between the range of an α-particle with energy, E_o, and the range of an α-particle with energy, E_α, i.e.,

$$t = R(E_o) - R(E_\alpha)\,. \qquad (2)$$

The computer code *SRIM: The Stopping and Range of Ions in Matter* (Ziegler, 1998) was used to calculate range. SRIM is a group of programs that calculates the stopping powers and ranges of ions up to 2 GeV/amu into matter, using a quantum mechanical treatment of ion-atom collisions. The program used to calculate range is called *TRIM*, which performs Monte Carlo transport calculations of ion interactions with multi-layer complex targets. Target materials are entered in TRIM by element up to atomic number 92, uranium; therefore, UO_2 was entered as the target material, being the closest to PuO_2. The density of UO_2 entered in TRIM was the same as that for PuO_2, i.e., 11.46 g/cm^3.

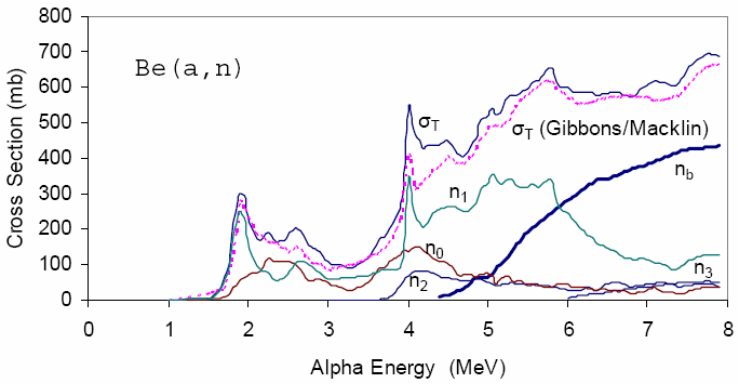

Figure 2. Cross Section σ_T for the Be(α, n) Reaction.

For the initial α-particle energy of 5.6 MeV and the threshold energy for the Be(α, n) reaction of 1.5 MeV, the ranges in PuO_2 calculated by TRIM are 12.85 μm and 2.68 μm, respectively. Thus, the distance t through which the energy of the α-particle falls from its initial energy to the threshold energy is 10.17 μm. Therefore, all α-particles produced more than 10.17 μm from the surface of the PuO_2 particle regardless of its direction, and some α-particles produced within 10.17 μm of the surface, depending on its direction, will not contribute to the Be(α, n) neutron source.

The information presented in Fig. 2 for σ_T shows clearly that there are three, distinct regions of interest. The first of these is in the region between 0 and about 1.5 MeV. The 1.5 MeV in this case represents the threshold energy, and, as was noted above, no neutrons are produced in beryllium from α-particles with energies less than 1.5 MeV. Therefore, this first region can be ignored entirely. The second region of interest is the region between 1.5 and 3.2 MeV. Neutrons produced as a result of α-particles with an energy in this region are the result of quantum-mechanical *tunneling*, because the α-particles do not have enough kinetic energy to overcome the height of the Coulomb barrier of the beryllium nucleus. Alpha-particles with energies in this range must tunnel *through* the Coulomb barrier before they can produce a neutron. The third region of interest is the region between 3.2 MeV and the initial energy of 5.6 MeV. Since the height of the Coulomb barrier for the beryllium nucleus is about 3.2 MeV, all α-particles with energies greater than 3.2 MeV can easily produce neutrons, because all reactions are now energetically favored. Consequently, the cross section increases beginning at about 3.2 MeV, exhibiting a steep leading edge, as shown in Fig. 2, at 4.0 MeV. Because of this steep increase, we elected to use the energy regions between 1.5 and 4.0 MeV, and between 4.0 and 5.6 MeV, for all additional calculations described below.

Thus, in addition to the range of 5.6 and 1.5 MeV α-particles in PuO_2, it now also becomes desirable to know the range of 4.0 MeV α-particles, which is 8.20 μm as calculated with TRIM. The distance t through which the energy of the α-particle falls from its initial energy to this intermediate energy is 4.65 μm.

Derivation of the α-Particle Escape Fraction, F_{esc}

Consider a spherical PuO_2 particle of radius $R_{particle}$; an α-particle originating at radius r_α within the PuO_2 particle, $0 \le r_\alpha \le R_{particle}$; and an initial energy E_o of the α particle, which corresponds to a range, R_α, in PuO_2.

The fraction of α-particles that escape the PuO_2 particle depends on both the point of origin and the direction of the α-particle. Figure 3 shows an α-particle produced at r_α, and the possible stopped locations as indicated by the sphere with radius equal to the range, R_α. If r_α is within the range, R_α, of the surface of the PuO_2 particle, and if the direction of the

α-particle is within the hatched volume, the α-particle will escape.

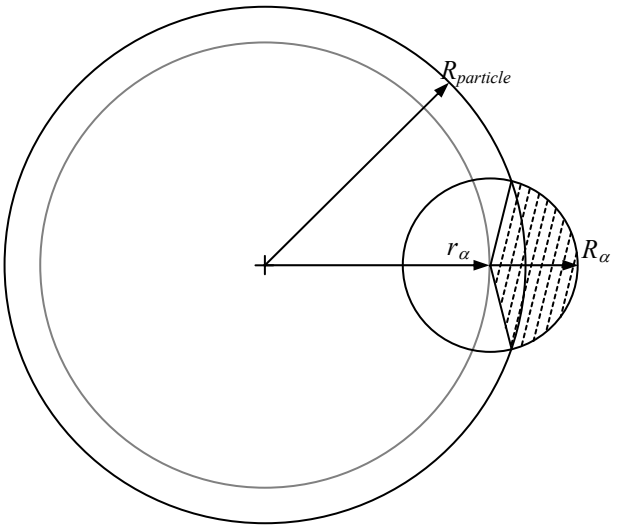

Figure 3. Schematic of a Spherical PuO_2 Particle Showing the Point of Origin of the α-Particle.

The hatched volume is a piece of the sphere with radius R_α, i.e., it is the portion of the cone formed within the sphere when the hatched area in Fig. 3 is rotated about its centerline. The probability that an α-particle will escape, P_{esc}, for $r_\alpha > R_{particle} - R_\alpha$, is equal to the ratio of the volume, $V_{hatched}$, of the hatched fraction of the sphere in Fig. 3 with radius equal to the range, R_α, to the total volume of the sphere with radius R_α, i.e.,

$$P_{esc} = \frac{V_{hatched}}{\frac{4}{3}\pi R_\alpha^3} . \tag{3}$$

The hatched volume is given by

$$V_{hatched} = \int_0^{\phi_0}\int_0^{2\pi}\int_0^{R_\alpha} \rho^2 \sin\phi \, d\rho \, d\theta \, d\phi , \tag{4}$$

where (ρ, θ, ϕ) are spherical coordinates for radius, azimuthal angle, and polar angle, respectively, and ϕ_0 is the polar angle of the hatched volume, as shown in Fig. 4.

Carrying out the integration gives

$$V_{hatched} = \tfrac{2}{3}\pi R_\alpha^3 \left(1 - \cos\phi_0\right) . \tag{5}$$

Substituting the expression for $V_{hatched}$ from Eq. (5) into Eq. (3) gives

$$P_{esc} = \tfrac{1}{2}\left(1 - \cos\phi_0\right) . \tag{6}$$

Note that if $R_\alpha > 2R_{particle}$, P_{esc} is 1.0, i.e., all α-particles escape regardless of where in the PuO_2 particle they originate. For $r_\alpha \le R_{particle} - R_\alpha$, P_{esc} is 0.

Because the angles ϕ_0 and ϕ_1 are supplementary, i.e., ϕ_0 is equal to $\pi - \phi_1$, solving for ϕ_1 will give ϕ_0. The angle ϕ_1 can be determined using the law of cosines as a function of the radius of the PuO_2 particle, $R_{particle}$, the location of the origin of the α-particle, r_α, and the range of the α-particle in the PuO_2 particle, R_α, i.e.,

$$\cos\phi_1 = \frac{-R_{particle}^2 + r_\alpha^2 + R_\alpha^2}{2 r_\alpha R_\alpha} . \tag{7}$$

This equation is valid for $r_\alpha > R_{particle} - R_\alpha$.

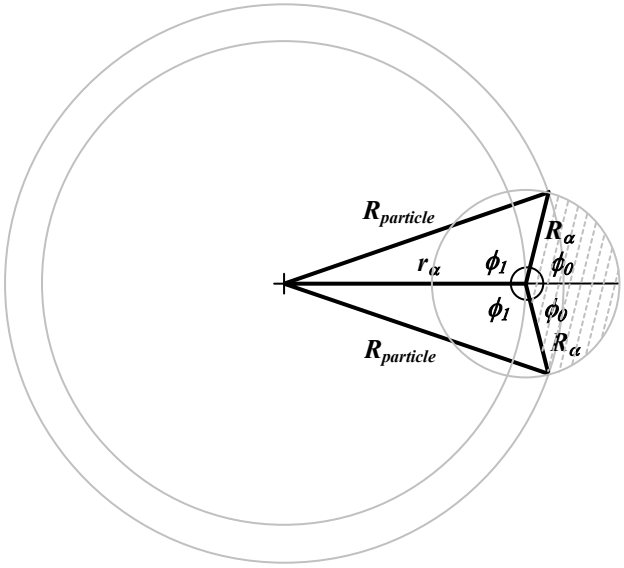

Figure 4. Angles – ϕ_0 and ϕ_1.

A property of the cosine function is that

$$\cos A = -\cos\left(\pi \pm A\right) . \tag{8}$$

From this property, and the fact that the angles ϕ_0 and ϕ_1 are supplementary, the following is obtained:

$$\cos\phi_0 = \cos\left(\pi - \phi_1\right) = -\cos\phi_1 . \tag{9}$$

Substituting the expression for cos ϕ_1 from Eq. (7) into Eq. (9), and substituting the resulting expression for cos ϕ_0 into Eq. (6) gives the probability that an α-particle will escape in terms of the known values, $R_{particle}$ and R_α, and the variable r_α, i.e.,

$$P_{esc} = \frac{1}{2}\left(1 - \frac{R_{particle}^2 - r_\alpha^2 - R_\alpha^2}{2 r_\alpha R_\alpha}\right) . \tag{10}$$

The escape fraction, F_{esc}, is the ratio of the number of α-particles that escape to the total number of α-particles that are produced in the PuO_2 particle. Because the number of α-particles that escape is a function of the escape probability, P_{esc}, which itself is a function of the position, r_α, where the α-particles originate within the PuO_2 particle, the escape fraction, F_{esc}, is an integral quantity.

The total number of α-particles that are produced in the PuO_2 particle is simply the product of the volume of the PuO_2 particle, the mass of plutonium per unit volume, and the α-particle generation rate per unit mass from Table 3. The

number of α-particles that are produced within a differential shell between r_α and $r_\alpha + dr_\alpha$ that escape the PuO_2 particle is the product of the escape probability, P_{esc} at r_α, the volume of the differential shell dV, the mass of plutonium per unit volume, and the α-particle generation rate. Because both the mass of plutonium per unit volume and the α-particle generation rate per unit mass are constants that appear in both the numerator and the denominator of the escape fraction, F_{esc}, these factors cancel, and F_{esc} is given as

$$F_{esc} = \frac{\int P_{esc}\, dV}{\int dV} = \frac{\int_0^{R_{particle}} P_{esc}\, dV}{\frac{4}{3}\pi R_{particle}^3}. \qquad (11)$$

The integration in the numerator is carried out over the entire PuO_2 particle, from the center to the surface. However, because P_{esc}, the probability that an α-particle will escape, is 0 for $r_\alpha \le R_{particle} - R_\alpha$, the integral is non-zero only for r_α between $R_{particle} - R_\alpha$ and $R_{particle}$, and F_{esc} reduces to

$$F_{esc} = \frac{\int_{R_{particle}-R_\alpha}^{R_{particle}} P_{esc}\, dV}{\frac{4}{3}\pi R_{particle}^3}. \qquad (12)$$

For a spherical PuO_2 particle, the volume, dV, of the differential shell between r_α and $r_\alpha + dr_\alpha$ is given by $4\pi r_\alpha^2\, dr_\alpha$. Substituting for P_{esc} and dV gives

$$F_{esc} = \frac{\int_{R_{particle}-R_\alpha}^{R_{particle}} \frac{1}{2}\left(1 - \frac{R_{particle}^2 - R_\alpha^2 - r_\alpha^2}{2 r_\alpha R_\alpha}\right) 4\pi r_\alpha^2\, dr_\alpha}{\frac{4}{3}\pi R_{particle}^3}. \qquad (13)$$

Carrying out the integration and simplifying then gives

$$F_{esc} = \frac{3}{4}\frac{R_\alpha}{R_{particle}} - \frac{1}{16}\frac{R_\alpha^3}{R_{particle}^3}. \qquad (14)$$

Equation (14) gives the fraction of α-particles that are produced in the PuO_2 particle that escape in terms of the known values $R_{particle}$ and R_α. However, as was discussed above, those α-particles that escape with an energy below the Be(α, n) threshold energy of 1.5 MeV will not induce such reactions. Therefore, Eq. (14) must be partitioned into a fraction in which the energy of the α-particle escaping the PuO_2 particle is less than 1.5 MeV. Furthermore, as was also discussed above, it is desirable to partition the escape fraction at 4.0 MeV as well.

To determine the fraction of α-particles escaping the PuO_2 particle with an energy above 4.0 MeV, let $t_{4.0}$ be the distance through which the energy of an α-particle drops from 5.6 MeV to 4.0 MeV. Following Eq. (2), $t_{4.0}$ is the difference between the range at 5.6 MeV, *R(5.6)*, and the range at 4.0 MeV, *R(4.0)*, i.e.,

$$t_{4.0} = R(5.6) - R(4.0) = 4.65\ \mu\text{m}. \qquad (15)$$

Figure 5 shows that, for an α-particle originating at r_α, if r_α is within $t_{4.0}$ of the surface of the PuO_2 particle, and if the direction of the α-particle is within the diagonally hatched volume, the α-particle will escape, and its energy will be between 4.0 and 5.6 MeV. It is observed that Fig. 5 and Fig. 3 are similar, except that the hatched volume in Fig. 5 is a piece of the sphere with radius $t_{4.0}$ instead of R_α, as in Fig. 3. Therefore, for some arbitrary energy, E_α, that is less than the initital energy, E_o, the expression for the fraction of α-particles escaping the PuO_2 particle with an energy above E_α is given by replacing R_α in Eq. (14) with t from Eq. (2), i.e.,

$$F_{esc}\left(E > E_\alpha\right) = \frac{3}{4}\frac{t}{R_{particle}} - \frac{1}{16}\frac{t^3}{R_{particle}^3}. \qquad (16)$$

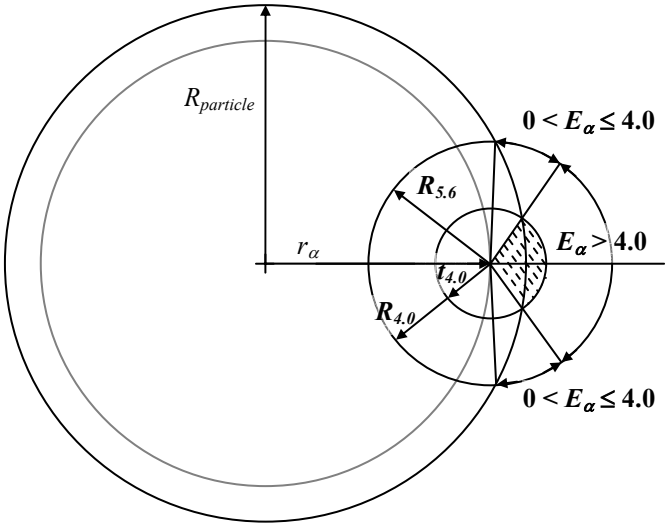

Figure 5. Schematic Showing the Probability of an α-Particle Escaping with an Energy Greater than 4.0 MeV.

Next, to determine the fraction of α-particles escaping the PuO_2 particle with an energy below 1.5 MeV, let $t_{1.5}$ be the distance through which the energy of an α-particle drops from 5.6 MeV to 1.5 MeV. Following Eq. (2), $t_{1.5}$ is the difference between the range at 5.6 MeV, *R(5.6)*, and the range at 1.5 MeV, *R(1.5)*, i.e., 10.17 μm. Therefore, the fraction of α-particles escaping the PuO_2 particle with an energy below 1.5 MeV is simply the difference between the fraction of α-particles that escape with any energy, from Eq. (14), and the fraction of α-particles that escape with an energy above 1.5 MeV, from Eq. (16), i.e.,

$$F_{esc}\left(E < 1.5\ \text{MeV}\right) = F_{esc}\left(\frac{R_\alpha}{R_{particle}}\right) - F_{esc}\left(\frac{t_{1.5}}{R_{particle}}\right). \qquad (17)$$

Lastly, the fraction of α-particles escaping the PuO_2 particle with an energy between 1.5 and 4.0 MeV is the difference between the fraction of α-particles that escape with an energy above 1.5 MeV, from Eq. (16) and $t_{1.5}$, and the fraction of α-particles that escape with an energy above 4.0 MeV, from Eq. (16) and $t_{4.0}$, i.e.,

$$F_{esc}\left(1.5\text{ MeV} < E < 4.0\text{ MeV}\right) = F_{esc}\left(\frac{t_{1.5}}{R_{particle}}\right) - F_{esc}\left(\frac{t_{4.0}}{R_{particle}}\right). \quad (18)$$

Using the above expressions for the escape fraction in these energy regions, the values of F_{esc} thus obtained are shown in Table 5. As can be seen in the table, all α-particles escape when the PuO_2 particle diameter is less than the 12.85 μm range.

Table 5. α-Particle Escape Fraction.

Diameter (μm)	F_{esc} ($0 < E_\alpha \leq$ 5.6 MeV)	F_{esc} ($0 < E_\alpha \leq$ 1.5 MeV)	F_{esc} ($1.5 < E_\alpha \leq$ 4.0 MeV)	F_{esc} ($4.0 < E_\alpha \leq$ 5.6 MeV)
0.35	1.00	0	0	1.00
0.7	1.00	0	0	1.00
1	1.00	0	0	1.00
1.3	1.00	0	0	1.00
1.8	1.00	0	0	1.00
2.3	1.00	0	0	1.00
3	1.00	0	0	1.00
4	1.00	0	0	1.00
5	1.00	0	0.0072	0.9928
6.5	1.00	0	0.11	0.89
8	1.00	0	0.23	0.77
10	1.00	0	0.35	0.65
13	0.9998	0.0658	0.4205	0.5135
17	0.92	0.13	0.39	0.40
20	0.83	0.13	0.35	0.34
25	0.70	0.13	0.30	0.28
31	0.59	0.11	0.25	0.22
37	0.50	0.098	0.21	0.19
44	0.43	0.085	0.18	0.16
53	0.36	0.072	0.15	0.13
63	0.30	0.062	0.13	0.11
75	0.25	0.052	0.11	0.093
88	0.22	0.045	0.093	0.079
105	0.18	0.038	0.078	0.066
125	0.15	0.032	0.066	0.056
149	0.13	0.027	0.055	0.047
177	0.11	0.023	0.047	0.039
210	0.092	0.019	0.039	0.033
250	0.077	0.016	0.033	0.028

BERYLLIUM INTERSECTION PROBABILITY

The third step in the process is to calculate, for an α-particle that escapes the PuO_2 particle, the probability that it will intersect a BeO particle.

If the α-particle escapes the PuO_2 particle in which it was produced, it will intersect an adjacent particle. There is a certain probability that the particle it intersects will be a BeO particle. Although a mixture of particles of two chemical compositions, each with its own particle size distribution, is an extremely complicated system, it is sufficient to estimate the beryllium intersection probability simplistically.

Two conceptual effects in a binary mixture of particles were considered:

- smaller particles that tend to fill in the gaps between the larger particles, pushing the larger particles up; and
- higher density particles that settle to the bottom, while the lower density particles rise to the top.

Based on the above two effects, one can imagine the smallest particles at the bottom of the can and the largest particles at the top. Within each layer of particles of nominally the same size, one can also imagine that the PuO_2 particles, being of greater density, settle at the bottom of the layer, and the BeO particles rise to the top of the layer. Such a structure would have a lower (α, n) neutron source than one in which the particles are uniformly mixed, regardless of size or density, and it would likely only be attained after the application of a vibrational force for a sufficient time. Therefore, the segregation of particles by density is neglected, and segregation only by size is considered; i.e., the BeO and PuO_2 particles are assumed to be uniformly mixed in each size bin. The beryllium intersection probability in this case is estimated to be the ratio of the number of BeO particles in the size bin to the total number of BeO and PuO_2 particles in the size bin. Thus, the probability that an escaped α-particle intersects a BeO particle is a function of both the PuO_2 and BeO particle size distributions.

Because the beryllium is a contaminant in the plutonium calcining process, there are no data on the particle size distribution of the BeO particles after calcination. However, the BeO particle size distribution is a significant factor in calculating the dose rate from (α, n) reactions. Note that, if the BeO particle size distribution is assumed to be the same as the PuO_2 particle size distribution, the beryllium intersection probability is the same for all size bins; i.e., it assumes a uniform mixture of all particles regardless of size or density, and is simply the ratio of the number of all BeO particles to the number of all particles. Gaussian (normal) particle size distributions were also considered, with average BeO particle sizes of 15, 20, and 25 μm, and standard deviations equal to the square root of the average, i.e., 3.9, 4.5, and 5 μm, respectively. Although, given the lack of data, the choice of BeO particle size distribution is entirely arbitrary, it does serve as an example that a mixture of BeO particles and PuO_2 particles that does not exceed the dose rate limits of 10 CFR 71.47 can be modeled. The uncertainty, however, of such an approach does place a greater reliance on the post-loading package dose rates than before.

PROBABILITY OF A Be(α, n) REACTION

Once the number of α-particles that intersect a BeO particle is known, the fourth step in the process is to calculate the probability that an α-particle moving through BeO will undergo an (α, n) reaction with beryllium.

Because an α-particle is much more likely to undergo interactions with the atomic electrons of the target material than the nuclei, most of the α-particles simply are stopped in the target without undergoing a nuclear reaction. Even for an idealized case of a beam of 5.6 MeV α-particles on a thick

beryllium target, only about 85 nuclei per million α-particles will undergo an (α, n) reaction (Anderson and Hertz, 1971).

The probability that an α-particle will move through a given thickness of BeO *without* undergoing an (α, n) reaction with an atom of beryllium, $P_{no\ (\alpha, n)}$, is given by

$$P_{no\ (\alpha,n)} = e^{-N\sigma x}, \qquad (19)$$

where,

N = the atom density of Be in BeO,
σ = the cross section of the Be(α, n) reaction, and
x = the thickness of BeO.

The atom density of Be, N_{Be}, in BeO is given by

$$N_{Be} = N_{BeO} = \frac{\rho_{BeO} N_A}{A_{BeO}}, \qquad (20)$$

where,

N_{BeO} = the molecular density of BeO (Note: From the stoichiometry, there is one atom of Be for every molecule of BeO; hence, the atom density of Be is equivalent to the molecular density of BeO.);
ρ_{BeO} = the mass density of BeO, 3.01 g/cm^3;
N_A = Avogadro's number, 6.02×10^{23} atoms or molecules per mole; and
A_{BeO} = the molecular weight of BeO, 25.01158 g/mol.

Substituting the above values gives an atom density of 7.24×10^{22} Be atoms/cm^3.

As shown in Fig. 2, the cross section, σ, of the Be(α, n) reaction is a function of energy. The energy of the α-particle at a given location in a BeO particle is a function of both the distance traveled within the BeO particle and the distance traveled within the PuO_2 particle, which, in turn, depends on both the position within the PuO_2 particle at which the α-particle is produced, and the direction of travel of the α-particle. To simplify the problem, an average cross section is used. The average cross section of the Be(α, n) reaction would most accurately be calculated using the energy-dependent flux of α-particles in the BeO particle as a weighting function. However, an equation for the energy-dependent flux of α-particles in the BeO particles is not readily available. For purposes of this paper, therefore, which is to provide an example of a model demonstrating that mixtures of BeO and PuO_2 particles can exist with dose rates below the dose rate limits of 10 CFR 71.47, it is sufficient to use an estimate of the average cross section based on a visual inspection of Fig. 2.

As was noted above in the *Range, Initial Energy, and Threshold Energy* section, our primary interests are in the energy regions between 1.5 and 4.0 MeV, and between 4.0 and 5.6 MeV, respectively. Because of these two distinct energy regions, it is appropriate to estimate the probability of an (α, n) reaction in each energy region separately, using a different average cross section for each region. Over the energy range from 4.0 MeV to the α-particle's initial energy of 5.6 MeV, a visual inspection of Fig. 2 indicates the average value is about 500 mb. Similarly, over the energy range from 1.5 MeV to 4.0 MeV, the average value is about 175 mb.

The distance x in BeO required for the α-particle to drop below the (α, n) reaction threshold of 1.5 MeV depends on the energy of the α-particle entering the BeO particle. Of the α-particles that escape the PuO_2 particles, those α-particles produced very near the surface of the PuO_2 particles with a direction near the outward normal of the surface will lose very little energy within the PuO_2 particles, and they will travel the furthest distance in the BeO particle. Conversely, of the α-particles that escape the PuO_2 particles, those α-particles produced far from the surface of the PuO_2 particles, or with a direction far from the outward normal of the surface, will lose considerable energy within the PuO_2 particles, and they will travel the shortest distance in the BeO particle. Hence, x is a function of both the position within the PuO_2 particle at which the α-particle is produced, and the direction of travel of the α-particle.

Rather than attempting to calculate the energy-dependent flux of α-particles escaping the PuO_2 particles, it is again sufficient to simplify the problem by breaking it into the two energy regions described above for the cross section. It is conservatively assumed, therefore, that, if an α-particle escapes a PuO_2 particle with an energy between its initial energy of 5.6 MeV and the intermediate energy of 4.0 MeV, it will have lost no energy within the PuO_2 particle, i.e., it is assumed to have an energy equal to its initial energy of 5.6 MeV. It is also conservatively assumed that, if an α-particle escapes a PuO_2 particle with an energy between 4.0 MeV and the threshold energy of 1.5 MeV, it will have lost only a minimal amount of energy within the PuO_2 particle, i.e., it is assumed to have an energy equal to the intermediate energy of 4.0 MeV. Of course, α-particles that escape with an energy below 1.5 MeV do not contribute to the Be(α, n) reaction. Using this approach, the escape fraction as partitioned in the third through the fifth columns of Table 5 is utilized.

For some small size bins, x may be larger than the size of the BeO particle; however, using the value of x as defined allows for the possibility of the α-particle entering another BeO particle after leaving the first BeO particle. This assumption eliminates the position of the BeO particle relative to the direction of the α-particle as a factor, i.e., whether the α-particle is transported on a diameter through the center of the BeO particle, or whether it is transported on a chord that grazes the BeO particle and possibly escapes to enter a second particle. Similarly, an α-particle that is transported through a small PuO_2 particle may emerge and intersect a BeO particle. However, for purposes of this paper, it is again sufficient to simplify the problem and assume that, if an α-particle intersects a BeO particle, regardless of the size, the α-particle will travel the distance in BeO required for its energy to drop to the (α, n) threshold energy of 1.5 MeV. Similarly, an α-particle that intersects a PuO_2 particle, regardless of the size, is assumed to

travel the distance in PuO_2 required for its energy to drop to the threshold energy.

For α-particle energies of 5.6, 4.0, and 1.5 MeV, the ranges in BeO calculated with TRIM are 18.09, 11.24, and 3.58 μm, respectively. As discussed above in the *Alpha-Particle Escape Fraction* section, the distance x traveled by the α-particle between these energies in BeO is simply the difference in the ranges at these energies, i.e., 6.84 μm between 5.6 and 4.0 MeV, and 7.66 μm between 4.0 and 1.5 MeV.

The probability that an α-particle with an energy of 5.6 MeV moving through BeO will undergo an (α, n) reaction with Be is then

$$P_{(\alpha,n)}\left(E_\alpha = 5.6 \text{ MeV}\right) = \left(1 - e^{-N\sigma_1 x_1}\right) + e^{-N\sigma_1 t_1}\left(1 - e^{-N\sigma_2 x_2}\right), \quad (21)$$

where the subscript "1" refers to the upper energy region, i.e., between 4.0 and 5.6 MeV, and the subscript "2" refers to the lower energy region, i.e., between 1.5 and 4.0 MeV. Substituting 7.24×10^{22} Be atoms/cm^3 for N, 500 mb for σ_1, 6.84 μm for x_1, 175 mb for σ_2, and 7.66 μm for x_2 gives a value of 0.000034, or 34 (α, n) reactions per million α-particles.

Similarly, the probability that an α-particle with an energy of 4.0 MeV moving through BeO will undergo an (α, n) reaction with Be is

$$P_{(\alpha,n)}\left(E_\alpha = 4 \text{ MeV}\right) = 1 - e^{-N\sigma_2 x_2}. \quad (22)$$

Substituting for N, σ_2 and x_2 gives a value of 0.000010, or 10 (α, n) reactions per million α-particles. It is noted that a 5.6 MeV α-particle, which has 1.4 times as much energy as a 4.0 MeV α-particle, creates 3.4 times as many neutrons.

In the case of the simplifying assumptions described above, these probabilities are not dependent on the size bin.

THE TOTAL NEUTRON SOURCE

The Be(α, n) neutron source in each size bin is then the product of the α-generation rate, the α-escape fraction, the Be intersection probability, and the probability that an α-particle in Be will undergo an (α, n) reaction. The total Be(α, n) neutron source is the sum over all size bins.

The energy spectrum of the neutron source is also a function of the energy of the α-particle, but the effect is, at best, second order. Therefore, the energy spectrum used here is calculated with SOURCES (Wilson, 1999).

In addition to neutrons produced by the Be(α, n) reaction, a smaller number of neutrons are produced by spontaneous fission of the actinide isotopes and by (α, n) reactions with ^{17}O and ^{18}O. Because spontaneous fission is not dependent on the extent of mixing or particle sizes, and because oxygen is homogeneously mixed with plutonium at the atomic level, it is appropriate to use SOURCES to calculate the neutron source from these reactions. The total neutron source is then the sum of the neutrons produced by all these reactions.

DOSE CALCULATIONS

The dose rate from the total neutron source at the radial surface of the 9975 package is calculated with MCNP (Briesmeister, 2000) using the model of the 9975 package shown in the SARP (WSRC, 2003). The cumulative distributions of package dose rates, based on the 18 batches of historical PuO_2 particle size distributions from Rocky Flats, using the isotopic distribution for "Hanford 10-13% Pu-240" aged plutonium from the 3013 Standard, for three Gaussian BeO particle size distributions are shown in Fig. 6. The iterated masses of plutonium and beryllium, and the optimized dose rate for an average BeO particle size of 25 μm, for each of the 18 batches of PuO_2, are shown in Table 6.

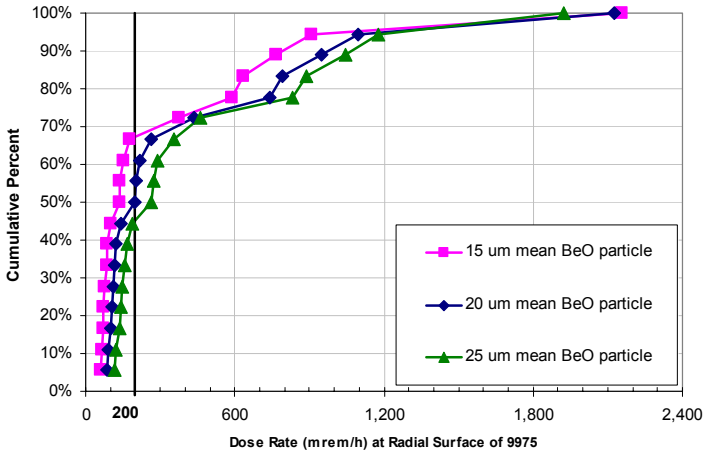

Figure 6. Cumulative Dose Rate Distribution for "Hanford 10-13% Pu-240" Plutonium.

It is noted that, when the BeO particle size distribution is assumed to be the same shape as the PuO_2 particle size distribution, the dose rates range from about 600 mrem/h to about 2,800 mrem/h for "Hanford 10-13% Pu-240" aged plutonium. Because these dose rates are not consistent with measurements, it was concluded that the BeO particle size distribution is not similar to the PuO_2 particle size distribution, and, therefore, this distribution is not shown in Fig. 6.

The largest uncertainties in the resulting dose rates arise from the uncertainty in the mass of beryllium actually present in the cans vis-à-vis the bounding value assumed in this estimate, and the uncertainty in the BeO particle size distribution, for which no measurements were available. Depending on the assumed BeO distribution, over half of the calculated dose rates are lower than regulatory limits.

Table 6. Dose Rates and Masses of Plutonium and Beryllium for 25 μm Average BeO Particles.

Batch	Dose Rate (mrem/h)	Mass (g) Pu	Mass (g) Be	Mass (g) BeO + PuO_2
0020ps	265	3,711	286	5,000
0024ps	830	3,407	410	5,000
0089ps	1,920	3,186	500	5,000
0695ps	885	3,372	424	5,000
1153ps	352	3,614	325	5,000
11608ps	458	3,575	341	5,000
1407psd	275	3,699	291	5,000
1490ps	1,041	3,311	449	5,000
1589ps	287	3,691	294	5,000
1856ps	1,176	3,258	471	5,000
2165ps	147	3,803	248	5,000
2201ps	189	3,788	254	5,000
2282ps	122	3,851	228	5,000
5501579ps	158	3,785	255	5,000
7013ps	165	3,802	249	5,000
can92ps	115	3,861	224	5,000
e7001psd	137	3,821	241	5,000
i6032ps	142	3,817	242	5,000

CONCLUSIONS

The cumulative distribution of package dose rates, based on the 18 batches of historical PuO_2 particle size distributions, is shown in Fig. 6 for "Hanford 10-13% Pu-240" plutonium. The calculated dose rates for all batches range from about 50 mrem/h to about 2,200 mrem/h, with over 50% of the batches being less than the 200 mrem/h limit for public transportation. A more refined analysis would show that almost all of the batches would be less than 200 mrem/h, but some could exceed this limit as seen by the distribution shape. Without detailed characterization of the BeO particle size distribution, additional analysis would not remove the uncertainty in these calculations. Because the actual amount of beryllium contamination is likely to be much less than 500 g, the dose rates would be expected to be much lower than those shown here.

Based on the particle size distribution analysis of the 18 batches analyzed, it is also likely that most of the 3013 cans to be loaded in the 9975 Package will have dose rates that are less than the 200 mrem/h limit for the package surface. However, extra care will be required in performing, and verifying, the dose rate measurements at the surface of the package, prior to shipment.

REFERENCES

Anderson, M. E., and M. R. Hertz, *Nucl. Sci. Eng.*, v. 44, p. 437 (1971).

Briesmeister, J. F., Ed., *MCNP – A General Purpose Monte Carlo N Particle Transport Code, Version 4C*, LA-13709-M, Los Alamos National Laboratory, Los Alamos, New Mexico, 2000.

DOE, *Packaging And Transportation Safety*, Order 460.1B, U.S. Department of Energy, Washington, D.C., 2003.

DOE, *U.S. Department of Energy Certificate of Compliance for Radioactive Materials Packages*, Certificate Number 9975, Revision 11, U.S. Department of Energy, Washington, D.C., 2004.

DOE, *Stabilization, Packaging, and Storage of Plutonium-Bearing Materials*, DOE-STD-3013-2004, U.S. Department of Energy, Washington, D.C., September 2004.

Levin, E. M., and H. F. McMurdie, *Phase Diagrams for Ceramists, 1975 Supplement*, American Ceramic Society, Columbus, Ohio, 1975.

NRC, 10 CFR Part 71, "Compatibility With the International Atomic Energy Agency (IAEA); Final Rule," 60 F.R. 50248, September 28, 1995, as amended.

Shores, E. F., *SOURCES: A Code for Calculating Neutron Sources and Spectra*, presented at ICRS-10 / RPSD 2004 21st Century Challenges in Radiation Protection and Shielding, Funchal, Madeira, 9-14 May 2004.

Thorp, D. T., *Particle Size Distributions for Oxides Calcined to DOE STD-3013*, Rocky Flats Environmental Technology Site, Golden, Colorado, Email to S. Primeau, Eagle Research Group, Inc., June 27, 2001.

Wilson, W.B., et al., *SOURCES 4A: A Code for Calculating (α, n), Spontaneous Fission, and Delayed Neutron Sources and Spectra*, LA-13639-MS, Los Alamos National Laboratory, Los Alamos, New Mexico, 1999.

WSRC, *Safety Analysis Report for Packaging Model 9975 B(M)F-85*, WSRC-SA-2002-00008, Rev. 0, Westinghouse Savannah River Company, Aiken, South Carolina, 2003.

Ziegler, J. F., *SRIM: The Stopping and Range of Ions in Matter Instruction Manual*, 1998. http://www.srim.org.